PHYSICAL REVIEW B VOLUME 23, NUMBER 4 15 FEBRUARY 1981

# Trapping of nitrogen in Mo due to defects generated by 50–400-keV $H^+$ and $He^+$ ions

A. Anttila, J. Hirvonen, and M. Hautala
*Department of Physics, University of Helsinki, SF-00170 Helsinki 17, Finland*
(Received 5 March 1980)

The trapping property of nitrogen diffusing in polycrystalline molybdenum has been used to study the distribution of defects generated by 50–400-keV $H^+$ and $He^+$ bombardment. The nitrogen-implanted samples were annealed at $T = 600$ and 750 °C. The defect concentrations were studied with different $H^+$ and $He^+$ doses ranging from $10^{14}$ to $10^{18}$ ions/cm$^2$. Increasing the $H^+$ and $He^+$ prebombardment doses led to a strong increase in the trapping of nitrogen and to the rapid migration of nitrogen atoms to the damaged region before trapping. The nitrogen defect trapping was observed to be very steady. The depth distributions of trapped nitrogen were measured with the $(p,\gamma)$ resonance-broadening method. The theoretical defect distributions were calculated using Monte Carlo calculations along with the tabulated electronic stopping-power values and good agreement was found between the theoretical and experimental defect profiles. The modal ranges of the 50–400-keV $H^+$ and $He^+$ ions in Mo derived as indirect by-products of the defect measurements agree with the values obtained through the Monte Carlo calculations, where the tabulated data for electronic stopping is employed, but are 20–40 % shorter than those where the electronic stopping according to the theory of Lindhard, Scharff, and Schiøtt is used.

## I. INTRODUCTION

Recently, van Veen and Caspers[1] studied the interaction of nitrogen with vacancies in molybdenum using thermal helium desorption. They observed a new recovery stage at $T = 627$ °C and proposed it to be due to the dissociation of nitrogen-occupied monovacancies. In our earlier work,[2] where the annealing behavior of nitrogen-implanted, proton-irradiated molybdenum was studied in the temperature region $T = 700$–$900$ °C, a strong increase in solubility and a decrease in diffusion were observed even with the low proton-irradiation doses. In that work the $(p,\gamma)$ resonance-broadening method was used with the aid of which, due to the high reaction cross section of $^{15}N(p,\alpha\gamma)^{12}C$, small quantities of nitrogen can be detected, allowing the diffusion process to be followed easily step by step. By combining the information obtained in these two studies it seemed *a priori* that by using the trapping property of nitrogen, the actual defect distribution profile arising during the prebombardment, by, e.g., protons could be determined fairly reliably.

Protons and $He^+$ ions were selected as bombarding particles. The energy region was limited to below 400 keV mainly owing to restrictions in the measuring techniques. An additional reason was that we expected to obtain information about the ranges of low-energy protons and $\alpha$ particles in molybdenum; for these cases no stopping data have so far been reported in the literature, e.g., in the recent compilations of Ziegler[3] and Andersen and Ziegler.[4]

## II. EXPERIMENTAL PROCEDURE

Electrolytically polished polycrystalline $15\times20\times0.2$-mm$^3$ molybdenum samples were used in the measurements. The purity of the molybdenum was 99.98%, according to the manufacturer's (Metallwerk Plansee) statement. The samples were preannealed at 1000 °C *in* 10 $\mu$Pa *vacuo* after which proton or $\alpha$-particle irradiations were performed using the 100-kV isotope separator or the 2.5-MV Van de Graaff accelerator at the University of Helsinki. For control purposes half of the sample was always shielded from the irradiation beam. The $^{15}N$ implantations were performed from enriched nitrogen gas (90% $^{15}N$) at 60-keV energy. The two-directional sweeping system produced an overall homogeneity of at least 1% for the implanted area of $1\times2$ cm$^2$. The implanted $^{15}N$ fluence was $2\times10^{16}$ ions/cm$^2$ in all cases. The proton and $\alpha$-particle fluences varied from $10^{14}$ to $10^{18}$ ions/cm$^2$ and the energies used were 50, 100, 200, and 400 keV. All implantations were performed at room temperature and *in* 100 $\mu$Pa *vacuo*.

The concentration curves were measured using the narrow $E_p = 429$ keV ($\Gamma = 0.9$ keV) resonance of the $^{15}N(p,\alpha\gamma)^{12}C$ reaction. The $\gamma$ rays were detected with a $12.7\times10.2$ cm$^2$ NaI(Tl) crystal. The depth-resolving power of the method is 3 nm at the surface and the reproducibility was confirmed by repeating some of the measurements. For a more detailed description of the experimental arrangement the reader is referred to our earlier paper.[5]

## III. ANNEALING AND IRRADIATION MEASUREMENTS

In contrast to van Veen and Caspers,[1] who in their thermal helium desorption measurement annealed *in vacuo*, we have in our earlier diffusion work done the annealing in a flowing-argon atmosphere. Since in both these experiments the measurements were performed very near the surface,

 

the pressure difference can be significant. According to the recovery curve,[1] the nitrogen trapping is constant below 600 °C, whereas the nitrogen dissociated from vacancies above 700 °C. The accessible temperature region for the $(p,\gamma)$ resonance-broadening method is 500–700 °C. Thus the optimum temperature of 600 °C was selected for the measurement. An annealing time of 45 min was found to change sufficiently the concentration profile at 600 °C. Since it was expected that the vacancy concentrations could be high, rather high nitrogen implantations were used (1 at. % at maximum). The solubility limit of nitrogen in molybdenum at 600 °C is 0.01 at. %[2]; thus the implanted-nitrogen concentration exceeded the solubility limit by a factor of 100. In order to obtain the fluence dependence of the damage, proton fluences of $10^{14}$, $10^{15}$, $10^{16}$, $10^{17}$, and $10^{18}$ $H^+$ ions/cm$^2$ at $E_p = 100$ keV and $He^+$ fluences of $10^{15}$, $10^{16}$, and $10^{17}$ at $E_\alpha = 50$ keV were used. In Figs. 1 and 2 the effect of the prebombardment on the annealed nitrogen profiles is shown. It is evident that the doses below $10^{16}$ ions/cm$^2$ are not very suitable for the measurements but doses of $10^{16}$–$10^{18}$ ions/cm$^2$ are relevant. Higher doses than these cause blistering effects, which naturally destroy the desired trapping study. The curves corresponding to the low fluences are therefore omitted, besides which they would detract from the clarity of the figure. As can be seen in Figs. 1 and 2, the strong surface peak in the nitrogen profile occurs in spite of high-temperature vacuum annealings, showing that the peak is rather permanent. The reason that nitrogen stays on the surface of molybdenum is that the nitrogen migrates in molybdenum as single atoms, not in the molecular form ($N_2$). The adsorption energy 3.1 eV (Ref. 6) for a single nitrogen atom is remarkably higher than the binding energy 1.35 eV of nitrogen in a vacancy[1] and also higher than the migration energy 1.2 eV.[7] Accordingly, the surface peak should actually be permanent at a temperature of 600 °C and further, the integral of the measured $^{15}N$ concentrations as compared to the amounts originally implanted is steady. In addition to the surface peak another clearly noticeable point in Figs. 1 and 2 is that the migration of nitrogen atoms to the damaged region increases strongly as a function of prebombardment dose.

To deduce from the measurements such parameters as would give a clear description of the profiles is not a straightforward task. The reason is that there is no mathematical function available to describe the whole profile. Therefore, in the present study the main results are presented in the form of diagrams. Figure 3 illustrates a measurement where the energy dependences of the proton irradiations are studied. The energies are again 50, 100, 200, and 400 keV. In all cases the annealing temperature ($T = 600$ °C), time (45 min), and the dose ($1\times10^{16}$ ions/cm$^2$) were the same.

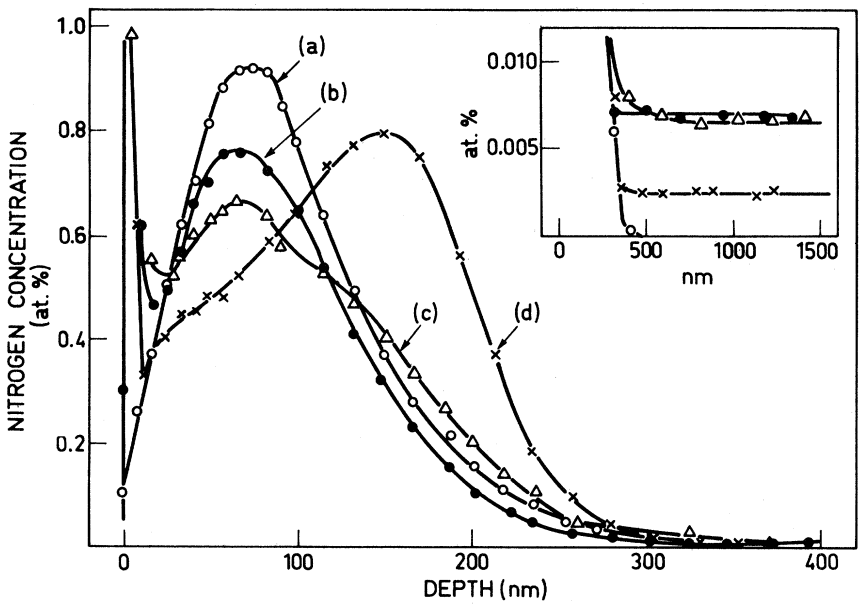


FIG. 1. Effect of 50-keV $He^+$ prebombardment on the concentration profiles of $^{15}N$ in annealing. Curve (a) is the profile of the 60-keV $^{15}N$ implantation before annealing and prebombardment and curve (b) after annealing at 600 °C for 45 min. The conditions in curves (c) and (d) are the same as in curve (b), except that before annealing irradiations of $10^{16}$ and $10^{17}$ ions/cm$^2$, respectively, were performed. The inset illustrates the solubility and diffusion in the tail part.

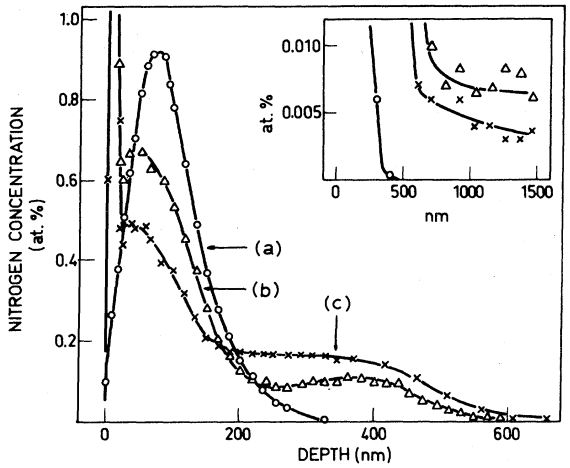


FIG. 2. Effect of 100-keV $H^+$ prebombardment on the concentration profiles of $^{15}N$ in Mo in annealing and prebombardment. Curve (a) is the profile of the 60-keV $^{15}N$ implantation before annealing. Curves (b) and (c) are the profiles after annealing at 600 °C for 45 min. The preirradiation doses were $10^{17}$ and $10^{18}$ $H^+$ ions/cm$^2$, respectively. The nonirradiated profile, omitted in the interests of clarity, is the same as in Fig. 1(b). The inset illustrates the diffusion and solubility in the tail part.

The range in the $E_p = 400$-keV case is so long that the filling of the vacancies is only partly achieved. In addition, as regards the measuring techniques, this case is difficult owing to the increasing nonresonant background. In Figs. 4 and 5 the effects of the annealing temperature and time on the trapping profiles are illustrated. As expected, it was observed that longer annealing times at 600 °C do not significantly change the profiles if the trapping has already occurred [e.g., curves (a) and (b) in Figs. 4 and 5]. On the other hand, increasing the temperature to 750 °C and annealing for 1 h in the 50-keV $He^+$ case, the whole distribution was displaced inwards and also changed somewhat in shape [Fig. 4(c)]. However, no nitrogen-vacancy dissociation happened, as might have been expected on the basis of the experiment of van Veen and Caspers.[1] Instead, the surface peak decreases clearly through evaporation and/or diffusion inwards. In the 100-keV $H^+$ case no inward migration of the profile took place, although in this case the profile of the surface part did alter. The height of the peak decreased somewhat and it became broader (see Fig. 5). The reason for this broadening is unclear, but one explanation might be nitride formation.

In Figs. 1–5 the inset in the upper right corner shows the nitrogen concentrations in the undamaged bulk material. The bulk material is actually undamaged, since the damage profiles descend very steeply, after which the diffusion occurs as a level "tube" (see insets). In all damaged cases the height of this tube is lower than that of the nonirradiated case 0.007% [Fig. 1, curve (b)]. The apparently lower solubility in the damaged cases is evidently due to the fact that sufficiently mobile nitrogen atoms were not able to penetrate through

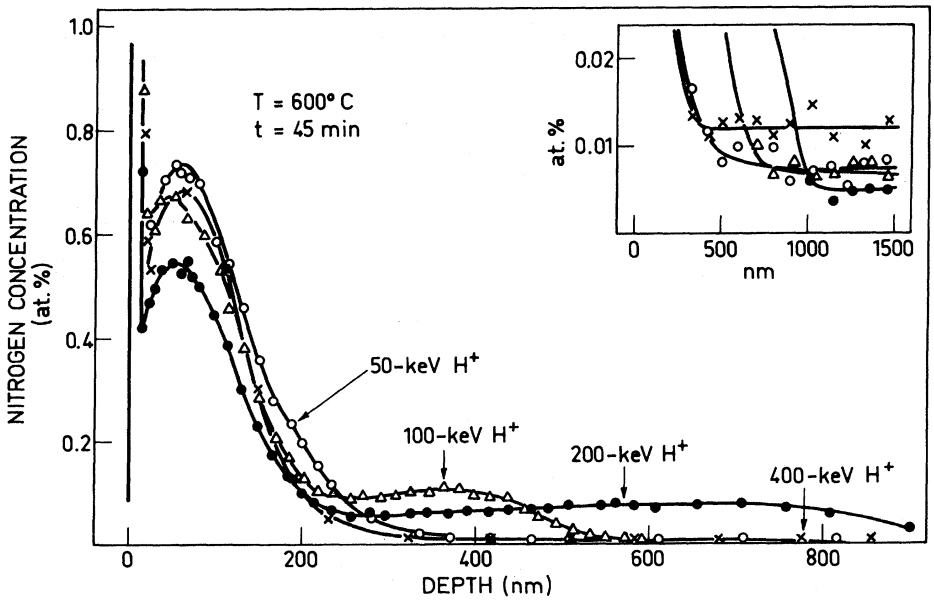


FIG. 3. Effect of 50-, 100-, 200-, and 400-keV $H^+$ prebombardment on the $^{15}N$ in Mo concentration profiles in annealing. In all cases the irradiation dose was $10^{17}$ $H^+$ ions/cm$^2$. The nonirradiated profile, omitted in the interests of clarity, is the same as in Fig. 1. The inset illustrates the solubility and diffusion in the tail part.

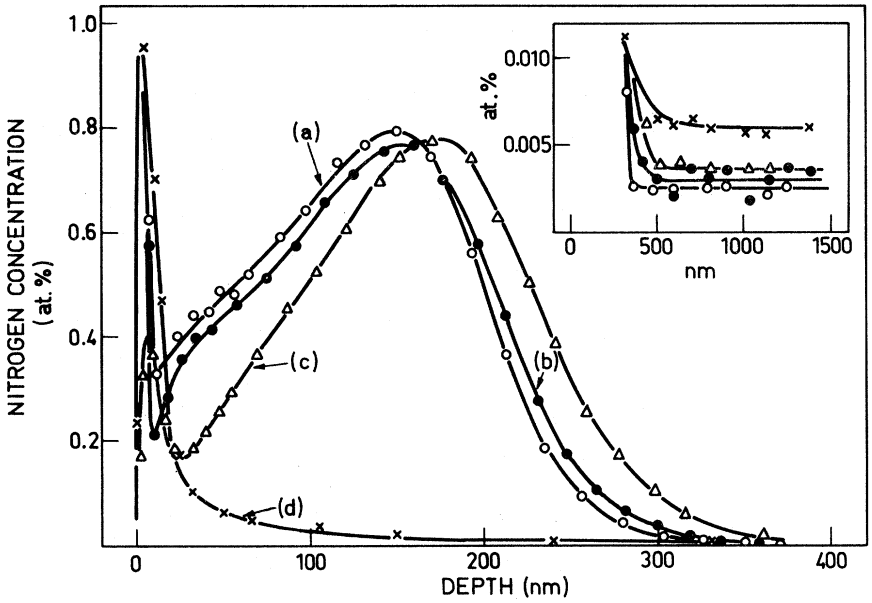


FIG. 4. Effect of the annealing time and temperature on the trapped $^{15}N$ in Mo profiles prebombarded with 50-keV $He^+$ ions. Curve (a) is the same as (d) in Fig. 1, $T = 600\,^{\circ}C$, $t = 45$ min, and the dose $= 10^{17}$ $He^+$ ions/cm$^2$. Curves (b) and (c) are the same as (a) except that the annealing was continued at 600 °C for 2 h and at 750 °C for 1 h, respectively. Curve (d) is an illustration from the nonirradiated case, $T = 750\,^{\circ}C$, and $t = 1$ h.

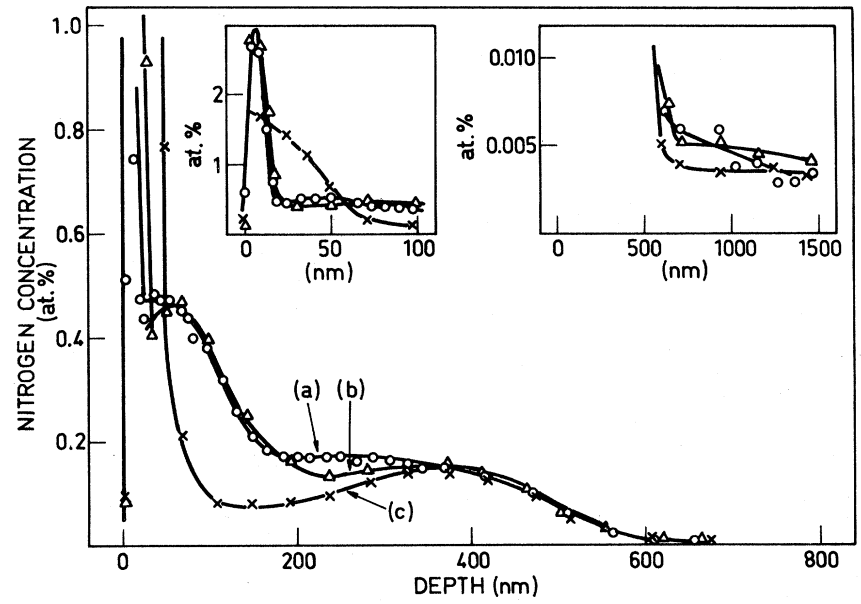


FIG. 5. Dependences of the trapped $^{15}N$ in Mo profiles on annealing time and temperature in the 100-keV $H^+$ irradiation case. Curve (a) is the same as (b) in Fig. 2, where $T = 600\,^{\circ}C$, $t = 45$ min, and dose $= 10^{17}$ $He^+$ ions/cm$^2$. Curve (b) is the same as (a) except that $t = 2$ h. Curve (c) is the same as (b) except that the annealing was continued at 750 °C for 1 h (cf. Fig. 1 for the nonirradiated profile). The insets illustrate the surface profiles and the solubility and diffusion in the tail part.

the trapped region. E.g., in the 50-keV $He^+$, high-dose case, the trapped region strongly blocked the nitrogen diffusion into the bulk specimen (Fig. 1).

## IV. DAMAGE DISTRIBUTIONS

### A. Theoretical calculations of range and Frenkel pair production

Stopping of the ions was determined using Monte Carlo calculations. In the program the scattering angle is calculated directly from the potential. The distance between the collisions and the impact parameter are derived on the assumption that the positions of the target atoms are Poisson-distributed. Thus, if $N$ is the number of atoms per unit volume, the distance between two successive collisions is determined by $-N^{-1/3}\ln R$, where $R$ is a random number $(0<R<1)$ and the impact parameter is chosen at random among 0 and $r_0$ defined by $\pi r_0^2 = N^{-2/3}$. The potential used in the calculation of the collisions is the mean of the potentials calculated from the Dirac-Fock electron distributions.[8] The electron stopping is treated as a continuous process. For a more detailed description of the program the reader is referred to our earlier paper.[8] In calculating the electronic stopping, both the theory of Lindhard, Scharff, and Schiøtt[9] (LSS) and the tabulations of Ziegler[3] and Andersen and Ziegler[4] were used. Being based on experimental systematics, the values given in the tabulations can be regarded as more reliable than the theoretical ones. Also it should be noticed that the validity of the LSS theory in the calculated energy region is questionable. In order to estimate the effect of the various potentials on the results the cases where H and He were assumed to be nonionized or completely ionized were calculated (the calculation method is described in Refs. 8 and 10), but it was found that the differences were insignificant at the relevant distances.

When such a light atom as H or He is the bombarding atom, a very close collision is needed, even at 50-keV energy, in order that a noticeable change in the direction of the ion takes place. E.g., in the helium case the impact parameter is 33 pm if the scattering angle is 1°, and is correspondingly 17 pm for protons. Therefore, to save computer time, it is necessary to disregard remote collisions. It was observed in an earlier paper[10] that it is possible by suitably choosing the impact parameter and the distance between successive collisions to take into account only those scatterings where the change in direction is greater than a selected angle (usually 1°). When an angle restriction of 2° was used, the number of the collisions in the simulations for the 400-keV H case decreased from 8000 to 200. The number of vacancy-interstitial pairs created in any collision was calculated using the modified Kinchin-Pease method. Accordingly, when the simulated ion gives an energy $T$ to a target atom, the number $\nu$ of the vacancy-interstitial pairs created is estimated by the relation

$$\nu(T)=0, \qquad T<E_d$$
$$\nu(T)=1, \qquad E_d\leq T<2E_d$$
$$\nu(T)=0.8T/2E_d, \qquad T>2E_d$$

where $E_d$ is the threshold energy for displacement. The value of 36 eV for $E_d$ was used.[11] The influence of the movement of the secondary ions on the distribution was neglected. This should not introduce any significant error, as their ranges are very small compared with the ranges of the bombarding ions.

As a by-product of the calculations it was found that the range and straggling values deviate considerably from those given in the book of Ziegler[3] and Andersen and Ziegler,[4] in spite of the same electronic stopping and not significantly different nuclear stopping. The discrepancy was found to be due to the correction made to the path length to obtain the projected range. For this correction, Ziegler used Schiøtt's analytical calculations,[12] which gave corrections 5–20% greater than those deduced in the present Monte Carlo calculations when the LSS stopping is used. However, using the stopping values given by Ziegler, the corrections are even 20–60% smaller than those used in the tabulations.

### B. Experimental and theoretical damage profiles

The modal range values of the experimental and theoretical damage profiles along with the theoretical modal ion ranges are given in Table I. In Figs. 6 and 7 a comparison between theory and experiment is shown. In calculating the experimental and theoretical damage profiles their modal range values were chosen to be equal. As can be seen in Figs. 6 and 7 the theoretical and experimental defect profiles are in good agreement. It seems that by taking into account the corrections as presented in the preceding section the tabulated stopping values of Ziegler[3] and Andersen and Ziegler[4] are in good agreement with the present ones (see Table I). On the other hand, the range values predicted by the LSS theory are clearly too long.

In Figs. 6 and 7 the calculated damage is given in units of displacement per ion/nm. The ratio of the defect yield generated by the $He^+$ ions compared to that of the protons is about 20. However, the corresponding experimental ratio is only about

TABLE I. Experimental and theoretical modal damage ranges ($\hat{R}_D$) of the 50–400-keV $H^+$ and $He^+$ ions in Mo and the corresponding modal ranges ($\hat{R}$).

| Ion | Energy (keV) | Present $\hat{R}_D$ | $\hat{R}$ [a] | $\hat{R}_D$ [a] | $\hat{R}$ [b] | $\hat{R}_D$ [b] |
|---|---|---|---|---|---|---|
| | | | (nm) | | | |
| $H^+$ | 50 | 180±30 | 230 | 190 | 360 | 290 |
| | 100 | 350±20 | 400 | 350 | 580 | 500 |
| | 200 | 650±50 | 780 | 720 | 920 | 820 |
| | 400 | >1500 | 1840 | 1770 | 1350 | 1250 |
| $He^+$ | 50 | 150±15 | 160 | 130 | 250 | 180 |
| | 100 | 240±20 | 280 | 230 | 450 | 390 |
| | 200 | 390±20 | 470 | 420 | 730 | 630 |
| | 400 | >500 | 750 | 680 | 1200 | 1100 |

[a] Calculated using Monte Carlo calculations and the corrected tabulation values of Ziegler (Ref. 3) and Andersen and Ziegler (Ref. 4) for the electronic stopping.

[b] Calculated using Monte Carlo calculations and the LSS theory (Ref. 9).

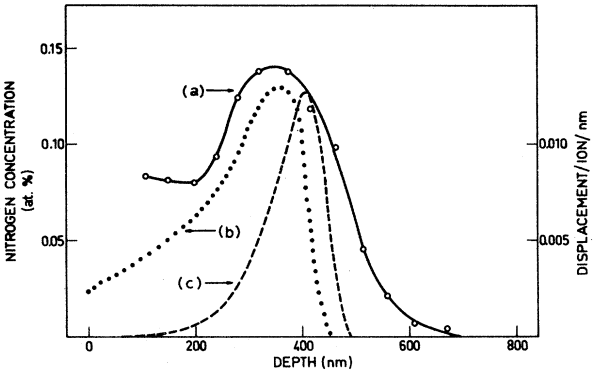


FIG. 7. Comparison of the the theoretical and experimental damage profiles in the 100-keV $H^+$ prebombardment case. Curve (a) is the same as (c) in Fig. 5. Curve (b) is the calculated damage profile. Curve (c) is the calculated range profile of the 100-keV protons.

5. Thus, as can be expected, the recombination in the high damage densities is more significant than in the low damage densities.

## V. DISCUSSION

The determination of the defect distributions generated by bombarding particles using a method based on the trapping of diffusing atoms and using a nuclear reaction for probing these diffusing atoms seems to be successful, when the conditions are suitably chosen. The damage profile can be determined directly and its evolution can be followed step by step. In the present work for probing nitrogen implanted into molybdenum the $(p,\gamma)$ resonance broadening has been used. The resolving power is good (3 nm for the N in Mo case) and also the sensitivity is rather good—the profile can be measured even on the 0.001-at. % level in a short time. On the whole, the nitrogen-migration process can be followed with sufficient accuracy. Another frequently used compatible method would be secondary-ion-mass-spectrometry (SIMS). However, it seems that SIMS fails to produce the correct depth profiles owing to the different erosion of various components. One of the most frequently used methods in connection with the diffusion process is a radiotracer method combined with some peeling method. However, nitrogen has no suitable isotope for such measurements, and, in addition, the diffusion rate at 600 °C is slow for the conventional radiotracer measurements. It seems that at present there are no other methods available with which light-mass-impurity distributions in heavy backings, such as the N-Mo combination, can be determined reliably in the subsurface region. In addition, there are many indirect methods which are useful for the study of some special properties in the defect process, but owing to the complexity of these processes they can sometimes lead to ambiguous conclusions. E.g., in the present work an unresolved question is the disagreement with the recovery curve obtained by van Veen and Caspers.[1] One explanation could be that the doses in the present work are higher than those used by van Veen and Caspers[1] and that the high doses can then generate vacancy clusters for which the dissociating energy is evidently higher.

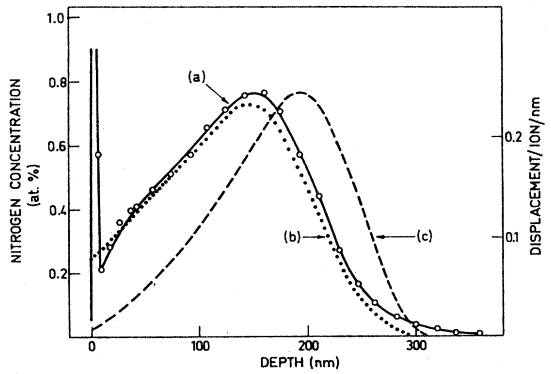


FIG. 6. Comparison of the theoretical and experimental damage profiles in the 50-keV $He^+$ prebombardment case. Curve (a) is the same as (b) in Fig. 4. Curve (b) is the calculated damage profile. Curve (c) is the calculated range profile of the 50-keV $He^+$ ions.

Although in the present work the trapping method has been applied to the particular case where the defects were generated by $H^+$ and $He^+$ ions, it is clear that defect distributions generated by other ions can be studied. In addition, it can be expected that corresponding recovery states to those in the N–Mo case occur in other element combina-

tions. It can also be expected that these recovery states occur in the region where the diffusion rate is of the same magnitude, and then further systematic defect study will be possible. One additional useful point is that, as a by-product of the defect study, rather reliable range values can be deduced which is especially important in the cases where no experimental data exist.

---

[1]A. van Veen and L. M. Caspers, Solid State Commun. 30, 761 (1979).
[2]A. Anttila and J. Hirvonen, Appl. Phys. Lett. 33, 394 (1978).
[3]J. F. Ziegler, *Helium: Stopping Powers and Ranges in All Elemental Matter* (Pergamon, New York, 1977).
[4]H. H. Andersen and J. F. Ziegler, *Hydrogen Stopping Powers and Ranges in All Elements* (Pergamon, New York, 1977).
[5]A. Anttila, A. Fontell, M. Bister, and K. B. Winterbon, Radiat. Eff. 33, 13 (1977).
[6]F. Reiter, in *Proceedings of the 9th Symposium on Fusion Technology*, edited by Commission of the European Communities (Pergamon, Oxford, 1976), p. 57.
[7]J. H. Evans and B. L. Eyre, Acta Metall. 17, 1109 (1969). (1969).
[8]M. Bister, M. Hautala, and M. Jäntti, Radiat. Eff., in press.
[9]J. Lindhard, M. Scharff, and H. E. Schiøtt, K. Dan. Vidensk. Selsk. Mat.—Fys. Medd. 33, No. 14 (1963).
[10]M. Hautala, Radiat. Eff., in press.
[11]P. Vajda, Rev. Mod. Phys. 49, 481 (1977).
[12]H. E. Schiøtt, K. Dan. Vidensk. Selsk. Mat.—Fys. Medd. 35, No. 9 (1966).